ACTA ASTRONOMICA
Vol. 38 (1988) pp. 375–399

Classical Cepheids: Their Distances and Space Distribution

by

Antoni Opolski

Wrocław University Observatory, Wrocław, Poland

Received February 15, 1988

ABSTRACT

A simplified method of calculating classical Cepheid distances is proposed. It is based on photometric data, without the use of the reddenings.

By means of results obtained in this way the following problems are discussed: Cepheid double and more numerous aggregates; Properties of the cluster and association Cepheids; The $\langle B-V\rangle_0-\log P$ and $\Delta V-\langle B-V\rangle_0$ relations in selected parts of the Galaxy.

1. Classical Cepheid Distances

The distances of classical galactic Cepheids are usually determined on the basis of P-L-C or P-L relations, reddenings, *e.g.* E_{B-V}, and interstellar extinction, *e.g.* $A_V = RE_{B-V}$. While solving these problems, we meet the difficulties arising from the facts that the *P-L-C* and *P-L* relations are not yet definitely established, and the reddenings, E_{B-V}, are known for a relatively small number of individual stars. But the distances of Cepheids, calculated by the surface brightness method by Gieren (1986), and the distances of the cluster Cepheids, given by Fernie and McGonegal (1983), may be used for working out the relation between Cepheid distances and directly observable photometric data, avoiding the above mentioned difficulties and making the calculation of Cepheid distances more straightforward.

We start with the generally used formulas and notations:

$$M_V = a\log P + b\langle B-V\rangle_0 + c, \tag{1}$$

$$\langle B-V\rangle_0 = \langle B-V\rangle - E_{B-V}, \tag{2}$$

$$\langle V\rangle_0 = \langle V\rangle - RE_{B-V}. \tag{3}$$

From these, we have the distance modulus:

$$\text{Mod} = \langle V \rangle_0 - M_V = \langle V \rangle - a \log P - b \langle B-V \rangle + (b-R) E_{B-V} - c \qquad (4)$$

and the logarithm of distance r in parsecs:

$$\log r = 0.2\,\text{Mod} + 1.00 = 0.2 \langle V \rangle - 0.2\,a \log P - 0.2\,b \langle B-V \rangle + \\ + 0.2(b-R) E_{B-V} - 0.2c + 1.00. \qquad (5)$$

From this formula it is evident that by means of the known values of r, $\langle V \rangle$, $\log P$, $\langle B-V \rangle$, and E_{B-V} it is possible to calculate – by the least squares method – the coefficients A, B, C, D in the equation:

$$\log r - 0.2 \langle V \rangle = A \log P + B \langle B-V \rangle + C E_{B-V} + D, \qquad (6)$$

and to use them in order to determine the distances r of Cepheids, for which the period P, and the photometric data, $\langle V \rangle$, $\langle B-V \rangle$, and E_{B-V} are known.

As the basic body of stars with known distances we have assumed 21 Cepheids listed in Table 1. Eleven of them denoted by G, have been taken from

Table 1
21 Cepheids with known distances.

	Star	log P	E_{B-V}	log r
FM	SU Cas	0.290	0.24	2.544
FM	EV Sct	.490	.64	3.230
G	SZ Tau	.498	.28	2.736
G	SS Sct	.565	.36	2.963
G	RT Aur	.571	.06	2.650
G	BF Oph	.609	.29	2.932
G	V482 Sco	.657	.34	3.035
FM	CF Cas	.688	.55	3.571
G	AP Sgr	.704	.19	2.968
G	V350 Sgr	.712	.33	3.008
FM	UY Per	.730	.91	3.410
FM	CV Mon	.731	0.75	3.301
FM	VY Per	.743	1.00	3.410
G	RV Sco	.783	0.38	2.895
G	BB Sgr	.822	.27	2.888
FM	U Sgr	.829	.43	2.842
FM	DL Cas	0.903	.51	3.270
G	TT Aql	1.138	.43	3.043
FM	WZ Sgr	1.339	.43	3.252
G	T Mon	1.432	.18	3.193
FM	SV Vul	1.653	0.41	3.420

a paper by Gieren (1986), and the ten cluster Cepheids from Fernie and McGonegal (1983), hereafter FM, taking into account the results published by Opolski (1985). According to FM, cluster Cepheids alone do not establish the *P-L-C* relation, only the *P-C* and *P-L* relations. Therefore, the addition of Gieren's stars should result in a better determination of the coefficients in Eq. (6). The periods and the photometric data, $\langle V \rangle$ and $\langle B-V \rangle$, have been taken from two catalogues: Schaltenbrand and Tammann (1971), hereafter denoted ST, and Moffett and Barness (1985), hereafter denoted MB. The results of the calculations are as follows:

photometry:	ST	MB
A	$+0.72 \pm 0.14$	$+0.73 \pm 0.12$
B	-0.42 ± 0.26	-0.43 ± 0.22
C	-0.16 ± 0.25	-0.19 ± 0.19
D	$+1.43 \pm 0.09$	$+1.47 \pm 0.08$
stand.dev.	0.038	0.035

On the basis of these quantities we may conclude that MB photometry gives somewhat more accurate values than the ST one. It is significant that in both systems the coefficient C of the reddening term $CE_{B-V} = 0.2\,(b-R)\,E_{B-V}$ is meaningless, having the error greater or equal to its value. Consequently, we have decided to omit this term, that is to assume $C = 0$ or $b = R$. With this change the solution for the same set of stars is:

photometry	ST	MB
A	$+0.808 \pm 0.033$	$+0.842 \pm 0.031$
B	-0.579 ± 0.040	-0.643 ± 0.041
D	$+1.481 \pm 0.037$	$+1.511 \pm 0.035$
stand.dev.	0.039	0.036

Now we see that, because of limited accuracy of all observational data used in these calculations, omitting the reddening term CE_{B-V} in Eq. (6) has resulted in an increase of the accuracy of the coefficients A, B, and D. The standard deviations remain nearly the same and correspond to 5 – 10% accuracy of the distance determination (Gieren 1986). These circumstances cause that it is possible to determine the Cephêid distances without any knowledge of their reddenings, which is an essential simplification of this problem. From the values of B it follows that the corresponding coefficient $b = -5B$, in the P-L-C relation (1), amounts $+2.90$ and $+3.22$.

On the basis of these considerations we have for ST photometry:

$$\log r = 0.2\,\langle V\rangle + 0.808\log P - 0.579\,\langle B-V\rangle + 1.481, \tag{7}$$

$$b = R = 2.90,$$

and as the P-L-C relation:

$$M_V = -4.04\log P + 2.90\,\langle B-V\rangle_0 - 2.405. \tag{8}$$

Similarly for BM photometry we have:

$$\log r = 0.2\,\langle V\rangle + 0.842\log P - 0.643\,\langle B-V\rangle + 1.511, \tag{9}$$

$$b = R = 3.22,$$

$$M_V = -4.21\log P + 3.22\,\langle B-V\rangle_0 - 2.555. \tag{10}$$

The differences between formulas for the two photometric systems, ST and MB, are due to the systematic differences between $\langle B-V\rangle_{ST}$ and $\langle B-V\rangle_{MB}$, stated by MB. The value $R = 3.22$ is more nearly correct than $R = 2.90$, so considering accuracy and correctness – the MB photometry surpasses the ST one. In spite of this, in the present paper we use the ST system because this catalogue comprises 266 stars denoted as type I, whereas the MB catalogue has only 104 Cepheids. We hope to get in this way a homogeneous set of distances for a relatively large number of stars.

The distances obtained by means of Eq. (7) have been verified and compared:

(1) For the 21 basic stars, Table 1, we have calculated the differences $\Delta \log r$ between the values of $\log r$ adopted from Gieren, G, and FM and listed in Table 1, and resulting from Eq. (7). Fig. 1 shows that up to $E_{B-V} \approx 1.00$ these differences do not depend on the reddenings which have been not used in this calculations. The same is true for $\Delta \log r$ resulting from $\log r$ (Eq. 9).

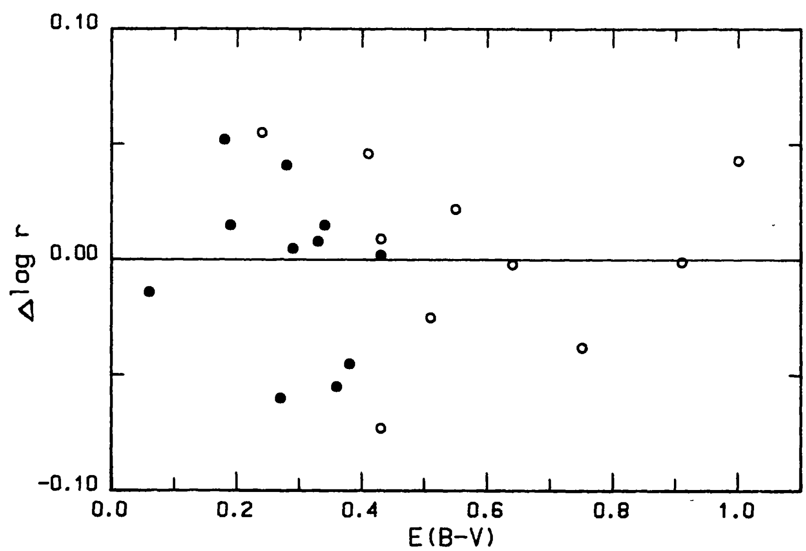

Fig. 1. The independence of $\Delta \log r$ on E_{B-V} for 21 stars with known distances from Table 1, ST photometry. Open circles represent FM stars, filled circles G stars.

(2) We have compared our distances r with r_{FH} of Fernie and Hube (1968) and with r_{IEN} of Ivanov *et al.* (1983). The comparison comprises 137 stars occurring in the three investigated collections that have distances r_{FH} and r_{IEN} determined to two decimals and have radial velocities V_r at least in one of the two above mentioned catalogues. Fig. 2 represents the comparison of our distances r with r_{FH}. In the range up to 6 kpc the agreement is satisfactory, but with considerable scatter. Fig. 3 shows that r_{IEN} are systematically smaller than our distances by about 8%, but the scatter of the points is much smaller than on Fig. 2.

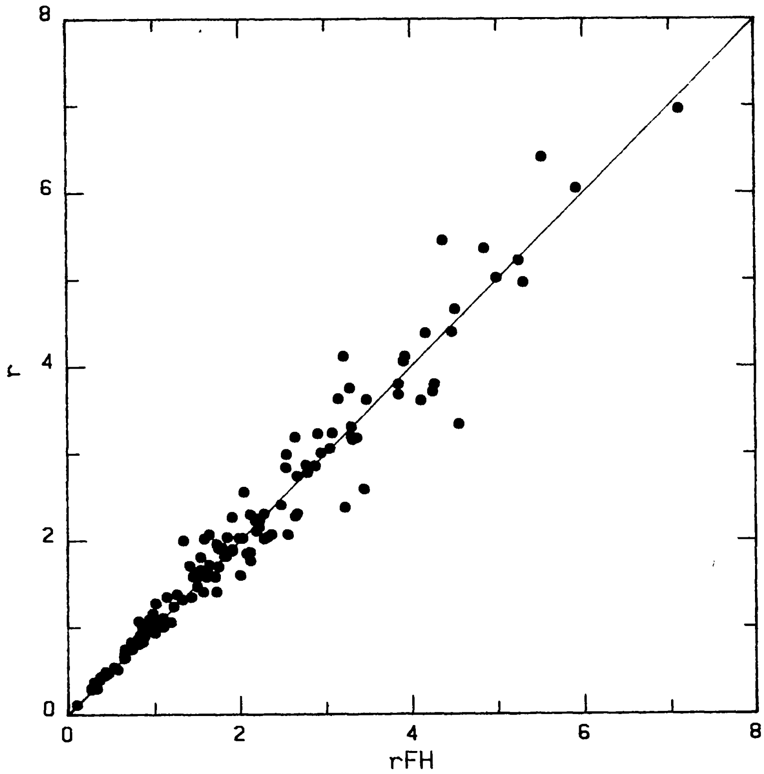

Fig. 2. The comparison of distances r resulting from Eq. (7) with r_{FH} from Fernie and Hube (1968), expressed in kpc.

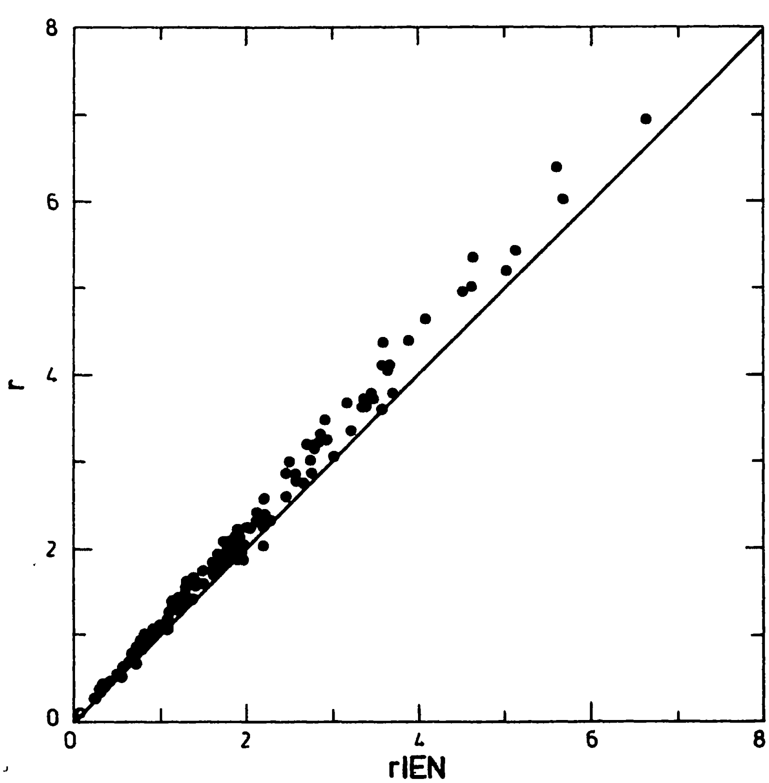

Fig. 3. The comparison of distances r resulting from Eq. (7) with r_{IEN} from Ivanov *et al.* (1983), expressed in kpc.

(3) A quite independent test of the three systems of distances may be done by calculating the Oort's galactic rotation constant A (Mihalas and Binney 1981):

$$Ar\cos^2 b \sin 2l = V_r + 9\cos b \cos l + 12\cos b \sin l + 7\sin b,$$

where b and l are stellar galactic coordinates. As distances r we used our values, r_{FH}, and r_{IEN}. After omitting 4 stars giving residuals greater than 40 km/s, we got from 133 common stars the following result:

distances	A km/s/kpc	stand.dev. km/s
r	11.07 ± 0.66	13.74
r_{FH}	11.14 ± 0.68	13.84
r_{IEN}	12.00 ± 0.73	13.87

From these values and accuracy of the results we see that in this case the three distance systems are nearly equivalent.

In the subsequent parts of this paper we present the results obtained from distances r calculated with the aid of Eq. (7) for the 266 stars denoted in the ST catalogue as type I and $-$I (Tables 5, 6, 7, 8 and 9).

2. Cepheid Space Distribution and the Spiral Structure of the Galaxy

Distances r, galactic longitude l, and galactic latitude b determine Cepheid rectangular coordinates X, Y, Z and the distances of the projections of stars on the galactic plane, a:

$$X = r\cos b \cos l, \qquad Y = r\cos b \sin l,$$

$$Z = r\sin b, \qquad a = r\cos b.$$

These data permit to show the distribution of the projections of stars on the galactic plane. Fig. 4 represents such a distribution for stars with $|Z| < 170$ pc. The nonuniformity visible in this figure is due to several factors: observational selection, interstellar absorption, and the natural arrangement of stars in space. Near the Sun, up to 1.0 kpc, the space is sparsely populated by Cepheids. The nearest 38 ones, with distances $r < 1$ kpc, are listed in Table 2. In this region the mean space density of Cepheids is 25 stars per kpc^3, and the mean separation between them amounts 350 pc.

The distribution represented on Fig. 4 gives no clear evidence that the investigated stars follow the spiral structure of our Galaxy. Taking into account the schematic diagrams of the spiral arms resulting from the radio data by Downes and Güsten (1982) it is possible to notice the following similarities:

In the directions $150° < l < 260°$, to galactic anticenter and along the

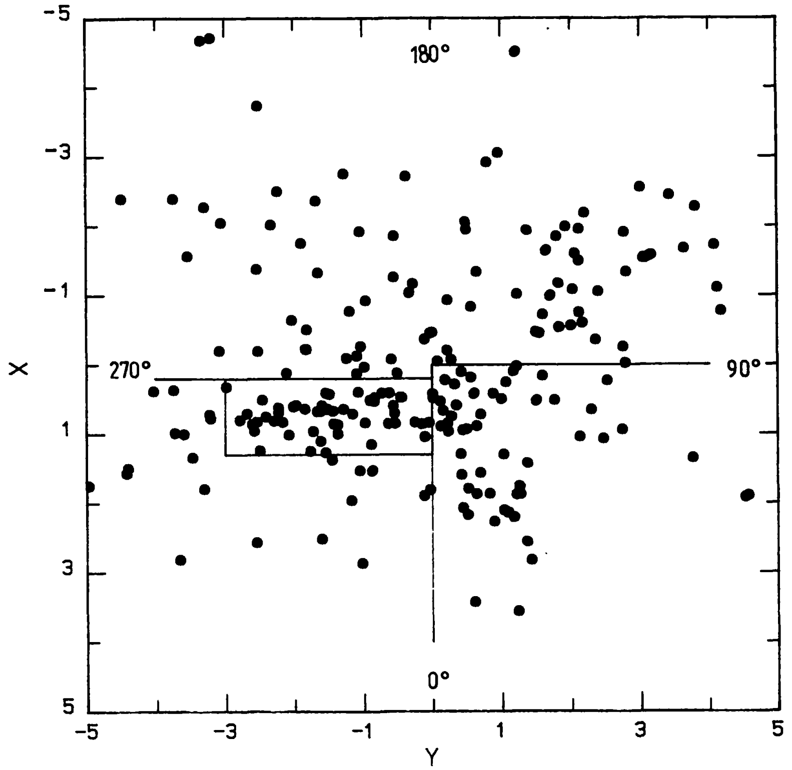

Fig. 4. Distribution of Cepheids in the galactic plane, $|Z| < 170$ pc. Coordinates X and Y in kpc. Limits of the interarm area and of the areas discussed in the paper are indicated.

Table 2
38 nearest Cepheids, $r < 1$ kpc.

No	Star	log P	r	No	Star	log P	r
1	α UMi	0.599	105 pc	20	U Aql	0.847	696 pc
2	δ Cep	.730	285	21	U Vul	.903	730
3	η Aql	.856	293	22	S Sge	.929	738
4	SU Cas	.290	309	23	S Cru	0.672	746
55	β Dor	0.993	361	24	Y Oph	1.234	807
6	ζ Gem	1.007	392	25	V Cen	0.740	820
7	X Sgr	0.846	422	26	T Cru	.828	838
8	FF Aql	.650	433	27	BF Oph	.609	845
9	DT Cyg	.398	439	28	TU Cas	.330	866
10	RT Aur	.572	462	29	RV Sco	.783	871
11	W Sgr	.881	478	30	V636 Sco	.832	871
12	SZ Tau	0.498	495	31	BB Sgr	.822	887
13	ι Car	1.551	527	32	AP Sgr	.704	897
14	Y Sgr	0.761	537	33	S TrA	.801	899
15	T Vul	.647	597	34	R Cru	.765	959
16	AH Vel	.626	605	35	AW Per	.810	967
17	R TrA	.530	649	36	SU Cyg	.585	975
18	AX Cir	.722	656	37	BG Vel	.840	985
19	U Sgr	0.828	681 pc	38	R Mus	0.876	994 pc

spiral arms, there is a smaller number of stars than in the other directions. This may be an analogy with the lack of dust and CO in these regions.

Worthy of notice is the interarm area 3 kpc long, 1.1 kpc broad and 340 pc thick, limited by the coordinates:

$$+200 \text{ pc} < X < +1300 \text{ pc}$$
$$-3000 \text{ pc} < Y < 0 \text{ pc}$$
$$-170 \text{ pc} < Z < +170 \text{ pc}$$

In Fig. 4 this area is visible as a strip with greater density of stars than the surroundings. In the cross-section X-Z (Fig. 5) the strip is visible end-on and the congestion of stars in this area is even more conspicuous. Fig. 6 shows the Y-Z section, side-on, of the same strip. Here we see that the stars form a convex band with the central part in greater Z than both ends. For 43 stars of the strip

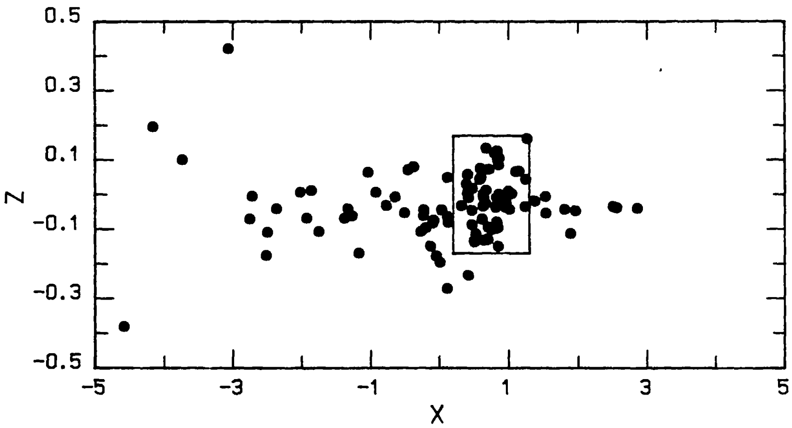

Fig. 5. End view of the interarm area. The X-Z crossection in kpc, $-3 < Y < 0$ kpc.

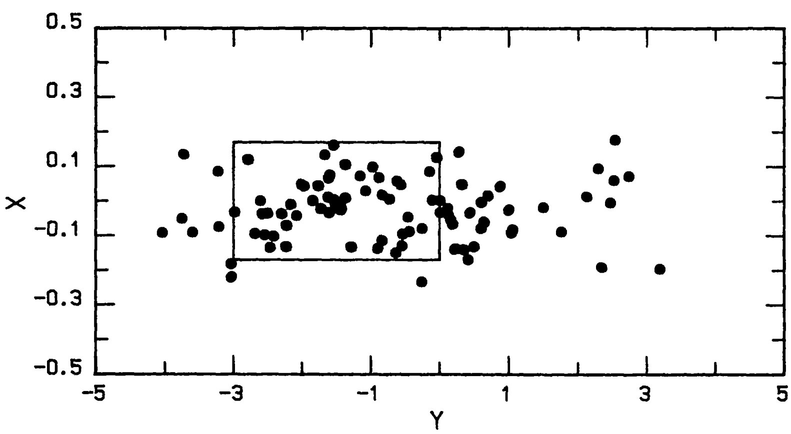

Fig. 6. Side view of the interarm area. The Y-Z crossection in kpc, $0.2 < X < 1.3$ kpc.

the individual reddenings E_{B-V} are published by Dean *et al.* (1978) and by Pel (1978). From these data we conclude that along the strip the reddenings increase slowly from $E_{B-V} = 0.20$ for $r = 0.5$ kpc to $E_{B-V} = 0.35$ for $r = 3$ kpc. That is, the space is here nearly free from the interstellar matter. The other properties of these interarm Cepheids are discussed in the next parts of this paper.

The main characteristics of Cepheid distribution perpendicular to galactic plane in the selected segments are as follows:

Segment directed towards galactic center, $-50° < l < +50°$: The stars are visible to 4 kpc with concentration at galactic plane $|Z| < 150$ pc. Majority of them has $Z < 0$. Reddening E_{B-V} reaches value 1.0 for $r = 2.0$ kpc and $Z = +100$ pc.

Anticenter segment, $150° < l < 220°$: Visibility of stars to 6 kpc, faint concentration at galactic plane, $|Z| < 500$ pc. Reddening $E_{B-V} = 0.6$ for $r = 2.0$ kpc.

Perpendicularly, $50° < l < 90°$, three stars are situated far from galactic plane, $Z > 400$ pc, and in the opposite segment, $210° < l < 270°$, two stars are far on the other side of the galactic plane, $Z < -400$ pc:

EP Cyg	$Z = 417$ pc,	$r = 6.84$ kpc
V 547 Cyg	486	8.20
V 924 Cyg	488	5.25
CU Mon	−597	8.25
CR Ori	−457	6.79

These stars may be suspected to be type II Cepheids with different Z and r.

3. Cepheid Double and Multiple Aggregates

Two stars nearby on the sky are also close to each other in the space when their distances are similar. The selection of such pairs and multiple aggregates were made by Efremow *et al.* (1981) and some comments on this subject were published by Opolski (1984). Now it is possible to repeat the same considerations using the newly calculated distances r.

Assuming that the distances of two stars, r_1 and r_2, are determined with the accuracy of 10% and their difference $\Delta r = |r_1 - r_2|$ with 14%, we regard that these stars form a pair when they have small differences of galactic coordinates $\Delta l = |l_1 - l_2|$ and $\Delta b = |b_1 - b_2|$ and when

$$\Delta r < 50 \text{ pc} + 0.14\ r, \tag{11}$$

where r is the mean distance of stars under consideration. In this way 32 pairs have been selected and listed in Table 3. Their angular separations:

$$\varrho = \sqrt{(\Delta l \cos b)^2 + (\Delta b)^2}$$

are distributed as follows:

ϱ:	0°0	0°5	1°0	1°5	2°0	2°5	3°0	3°5	4°0	4°5
N:	6	6	4	2	1	3	2	3	2	

The ϱ distribution has a maximum for the ϱ values smaller than 2°0. The corresponding space separations perpendicular to line of sight $d \doteq 17.5\varrho r$, where d is in pc, ϱ in degrees and r in kpc, show also the grouping of pairs for smaller values of d in the range $d < 80$ pc with a maximum near $d = 40$ pc:

d:	0	20	40	60	80	100	120	140	160 pc
N:	6	8	6	3	1	6	0	2	

Table 3
Cepheid pairs.

Star	log P	l^o	b^o	r_{kpc}	ϱ^o	d_{pc}	Star	log P	l^o	b^o	r_{kpc}	ϱ^o	d_{pc}
W Sgr	0.881	1.57	-3.97	0.45	4.21	32	VY Per	0.743	135.07	-1.68	2.32	0.89	38
X Sgr	0.846	1.16	+0.22	0.42			UY Per	0.730	135.94	-1.49	2.58		
WZ Sgr	1.339	12.11	-1.31	2.11	1.57	60	RX Aur	1.065	165.77	-1.29	2.01	3.22	116
AY Sgr	0.818	13.25	-2.39				Y Aur	0.587	166.75	-4.32	2.12		
Y Sgr	0.761	12.79	-2.13	0.54	2.39	26	TX Mon	0.940	214.14	-0.78	5.70	1.42	142
U Sgr	0.828	14.42	-3.95	0.68			XX Mon	0.737	215.52	-1.12	5.75		
BB Sgr	0.822	14.66	-9.00	0.89	1.39	23	VW Pup	0.632	235.36	-0.62	4.00	0.80	54
V350 Sgr	0.712	13.75	-7.95	1.00			X Pup	1.414	236.14	-0.78	3.68		
CK Sct	0.870	26.30	-0.46	2.34	0.86	36	AP Vel	0.495	262.98	-1.37	1.84	0.55	18
CM Sct	0.593	27.16	-0.44	2.40			RZ Vel	1.310	262.88	-1.91	1.83		
TY Sct	1.044	28.05	+0.12	2.90	0.18	8	DP Vel	0.739	275.38	-1.30	4.05	0.56	38
RU Sct	1.294	28.19	+0.24	2.50			FG Vel	0.810	275.52	-0.76	3.75		
V496 Aql	0.833	28.20	-7.12	1.06	6.12	112	UX Car	0.566	284.78	+0.16	1.59	0.99	27
SS Sct	0.565	25.17	-1.80	1.04			Y Car	0.561	285.64	-0.33	1.55		
TT Aql	1.138	36.00	-3.13	1.10	8.67	159	VY Car	1.278	286.55	+1.22	2.05	0.20	7
FM Aql	0.786	44.34	+0.90	1.00			SX Car	0.687	286.72	+1.33	2.10		
S Sge	0.923	55.16	-6.11	0.74	5.89	76	DY Car	0.670	288.81	-0.95	4.65	1.15	94
U Vul	0.903	56.02	-0.28	0.77			FN Car	0.661	289.61	-0.12	4.69		
X Vul	0.801	63.85	-1.28	1.12	3.90	72	CC Car	0.678	289.38	-1.59	5.27	0.42	39
SU Cyg	0.585	64.76	+2.51	0.98			WZ Car	1.362	289.29	-1.18	5.27		
SV Vul	1.654	63.94	+0.33	2.37	2.61	116	TZ Mus	0.694	296.62	-3.01	3.90	0.30	21
GH Cyg	0.893	66.54	-0.07	2.69			UU Mus	1.066	296.82	-3.23	4.14		
MW Cyg	0.775	70.93	-0.63	1.59	3.67	110	R Mus	0.876	302.10	-6.54	0.99	2.65	47
V383 Cyg	0.664	73.92	-2.76	1.83			S Mus	0.985	299.64	-7.52	1.04		
VZ Cyg	0.687	91.52	-8.51	1.96	1.63	54	AX Cir	0.722	315.83	-4.01	0.66	3.91	45
BG Lac	0.727	92.97	-9.26	1.86			R TrA	0.530	316.97	-7.75	0.65		
RR Lac	0.807	105.64	-2.01	2.26	0.40	15	S TrA	0.801	322.13	-8.22	0.90	1.12	19
Z Lac	1.037	105.76	-1.63	2.08			U TrA	0.410	323.23	-8.03	1.07		
V Lac	0.698	106.46	-2.58	1.91	0.10	3	V636 Sco	0.832	343.51	-5.21	0.87	3.98	61
X Lac	0.736	106.56	-2.56	1.62			RV Sco	0.978	346.98	-7.15	0.87		
BP Cas	0.797	125.36	+2.84	2.60	2.58	117	RY Sco	1.306	356.49	-3.41	1.90	3.26	106
AY Cas	0.459	127.93	+2.57	2.61			V500 Sco	0.969	359.02	-1.35	1.81		

Table 4
Cepheid complexes.

Star	log P	l^o	b^o	r_{kpc}	ϱ^o	d_{pc}
V493 Aql	0.475	32.99	-1.64	2.23		
V336 Aql	0.863	34.19	-2.13	2.26	1.30	51
SZ Aql	1.234	35.60	-2.04	2.16	1.41	56
CE Cas a	0.711	116.56	-1.01	3.45		
CE Cas b	0.651	"	"	3.51	0.00	0
CF Cas	0.688	116.58	-1.00	3.54	0.02	1
CG Cas	0.640	116.84	-1.31	3.42	0.40	25
GX Car	0.857	281.57	-3.06	2.52		
GZ Car	0.619	284.74	-1.95	2.78	3.36	148
UW Car	0.728	285.59	-1.75	2.31	0.87	38
UY Car	0.744	287.23	-3.22	2.34	2.20	97
UZ Car	0.716	287.28	-2.31	2.53	0.91	40
EY Car	0.459	288.00	-2.09	2.67	0.75	33
WW Car	0.670	288.20	+0.02	2.74	2.12	93
CY Car	0.630	289.49	-0.87	2.43	1.57	69
GH Car	0.758	290.93	-0.24	2.32	1.57	69
V419 Cen	0.741	292.06	+4.37	1.80		
GI Car	0.647	290.26	+2.55	1.70	2.56	78
AY Cen	0.725	292.57	+0.39	1.76	3.16	96
AZ Cen	0.507	292.79	-0.20	1.65	0.63	19
IT Car	0.877	291.47	-1.11	1.73	1.60	48
T Cru	0.828	299.44	+0.39	0.84		
R Cru	0.765	299.63	+1.07	0.96	0.71	11
S Cru	0.671	303.31	+4.44	0.75	4.99	74
VW Cru	0.721	300.91	-0.70	1.66		
AG Cru	0.584	301.67	+3.06	1.36	3.84	104
X Cru	0.794	302.28	+3.75	1.62	1.75	47
V496 Cen	0.646	304.36	+1.96	1.96		
MY Cen	0.574	305.26	+1.16	2.16	1.20	41
V378 Cen	0.810	306.11	+0.33	1.69	1.19	40

This kind of distribution may be interpreted as an evidence that among Cepheids exist wide pairs resulting from a common origin in a dust cloud. In this respect Cepheids differ from the visual double stars.

The same considerations may be repeated for triples and more numerous complexes defined similarly to the pairs discussed above (Table 4). The quantities ϱ and d denote the separations of neighbouring stars in the complexes. Their distribution have the same appearance as for pairs:

ϱ:	$0\overset{\circ}{.}0$	$0\overset{\circ}{.}5$	$1\overset{\circ}{.}0$	$1\overset{\circ}{.}5$	$2\overset{\circ}{.}0$	$2\overset{\circ}{.}5$	$3\overset{\circ}{.}0$	$3\overset{\circ}{.}5$	$4\overset{\circ}{.}0$	$4\overset{\circ}{.}5$
N:	3	3	5	4	4	2	2	2	0	1

d:	0	20	40	60	80	100	120	140	160 pc
N:	4	4	8	4	3	1	0	1	

In this case maximum of the d distribution occurs for $40 < d < 60$ pc.

4. Period-Colour-Mass Relations

177 investigated stars have reddenings E_{B-V} determined by Dean *et al.* (1978) and E_{V-B} by Pel (1978). These latter values can be transformed to E_{B-V} Dean's system. It is thus possible to change $\langle B-V \rangle$ to $\langle B-V \rangle_0 = \langle B-V \rangle - E_{B-V}$ and to construct the $\langle B-V \rangle_0 - \log P$ diagram (Fig. 7). In this figure the stars are spread on an elongated area, which represents the projection of the plane defined by the *P-L-C* relation in the three dimensional space $M_V - \log P - \langle B-V \rangle_0$.

The diagram $\langle B-V \rangle_0 - \log P$ can be completed by the constant photometric mass lines, $\mathcal{M}_{ph} =$ const., derived for stars in the second crossing of the instability strip by means of the following relations:

$$\log \mathcal{M}_{ph} = 0.155 - 0.355\, M_{bol} - 1.061\, \langle B-V \rangle_0 \tag{12}$$

according to Opolski (1984), Eq. 28.

$$M_{bol} = M_V + B.C. = M_V + 0.430 - 0.603\, \langle B-V \rangle_0, \tag{13}$$

according to van Genderen (1983).

As the *P-L-C* relation we accept Eq. (8) of this paper.

Eqs. (12), (13), and (8) determine the colour-period-mass relation:

$$\langle B-V \rangle_0 = 0.76 \log P - 0.53 \log \mathcal{M}_{ph} + 0.46, \tag{14}$$

and the constant mass lines on the $\langle B-V \rangle_0 - \log P$ diagram:

$$\langle B-V \rangle_0 = 0.76 \log P + \text{const.} \tag{15}$$

The large scatter of points in Fig. 7 makes it reasonable to determine only

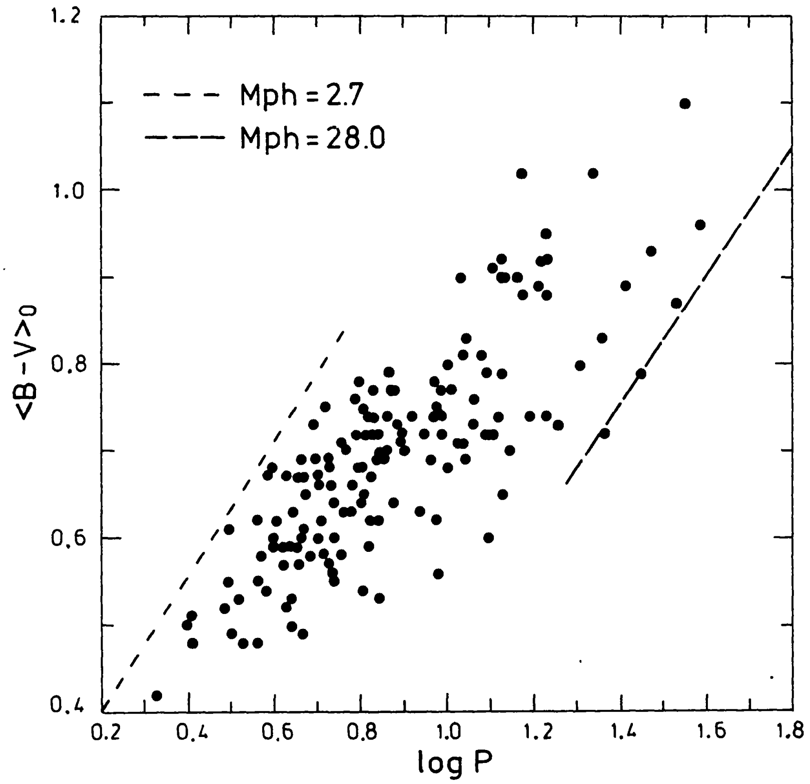

Fig. 7. The $\langle B-V\rangle_0$- $\log P$ diagram for Cepheids with known reddenings. The stars are between constant mass lines 2.7 and 28.0 $M_\odot$.

approximate mean relation:

$$\langle B-V\rangle_0 = 0.25 + 0.50 \log P. \tag{16}$$

For a given value of P, $\langle B-V\rangle_0$ vary in the range of 0.35. The stars are situated between mass lines $\mathcal{M}_{ph} = 2.7$ and 28 $M_\odot$.

The more conspicuous *P-C* relation exists for the following, selected groups of Cepheids:

Cluster and association Cepheids. The cluster and association Cepheids, proposed as distance indicators, are listed in the paper by Opolski (1985), where all details are given. In that paper we represent the differences

$$\Delta\mathrm{Mod} = \mathrm{Mod}_{\mathrm{FM}} - \mathrm{Mod}_0, \tag{17}$$

where $\mathrm{Mod}_{\mathrm{FM}}$ are the moduli published by FM and Mod_0 the moduli calculated by means of the accepted *P-L-C* relation. Now we may compare the values $\log r$ from Eq. (7) with $\log r_{\mathrm{FM}}$ resulting from $\mathrm{Mod}_{\mathrm{FM}}$:

$$\log r_{\mathrm{FM}} = 0.2\,\mathrm{Mod}_{\mathrm{FM}} + 1.000 \tag{18}$$

Only for T Mon we have changed $\mathrm{Mod}_{\mathrm{FM}} = 11.10$ to 10.96 according to Gieren

(1986). In this way we got

$$\Delta \log r = \log r_{FM} - \log r, \tag{19}$$

(see Table 5).

According to FM, cluster Cepheids determine only two-parameter relations: *P-C* and *P-L*. Therefore we calculated $\langle B-V\rangle_0 = \langle B-V\rangle - E_{B-V}$ using the reddenings E_{B-V} from Opolski (1985) and obtained the $\langle B-V\rangle_0 - \log P$ relation. Similarly from the formula:

$$M_V = \langle V\rangle - 5\log r + 5 - RE_{B-V} \tag{20}$$

Table 5

Cluster and association Cepheids.

Star	log P	log r	E_{B-V}	$\langle B-V\rangle_0$	M_V	Δ Mod	Δ log r	Δ $\langle B-V\rangle_0$
				typical cluster Cepheids				
SU Cas	0.290	2.489	0.24	0.48	-2.17	+0.18	+0.055	+0.02
EV Sct	.490	3.233	.64	.52	2.89	- .13	- .003	- .03
GU Nor	.538	3.246	.68	.62	2.80	- .03	(- .024))	+ .04
CE Cas b	.651	3.545	(.50)	(.64)	(3.19)	+ .08	+ .024	(.0)
CF Cas	.688	3.549	.55	.68	3.23	+ .13	+ .022	+ .03
CE Cas a	.711	3.537	(.54)	(.67)	(3.33)	+ .14	+ .034	(.0)
UY Per	.730	3.411	.91	.68	3.39	+ .09	- .001	+ .01
CV Mon	.731	3.341	.75	.62	3.58	- .30	- ,040	- .05
VY Per	.743	3.366	1.00	.64	3.54	+ .23	+ .044	- .04
U Sgr	.829	2.833	0.43	.71	3.70	- .04	+ .009	- .01
DL Cas	.903	3.296	.51	.71	4.02	- .29	- .026	- .04
S Nor	0.989	3.002	.22	.75	4.23	- .31	- .012	- .05
Y Sct	1.015	3.309	.75	.84	4.09	- .15	(- .053)	+ .02
X Cyg	.214	3.040	.23	.98	4.47	+ .19	(+ .018)	+ .08
VY Cyg	.278	3.312	.24	.95	4.81	+ .23	+ .062	+ .01
RZ Vel	.310	3.263	.32	0.89	5.13	- .03	+ .041	- .06
WZ Sgr	.339	3.325	.43	1.02	4.85	- ,26	- .073	+ .05
T Mon	.432	3.141	.18	.07	5.09	+ .29	+ .052	+ .06
SV Vol	.654	3.374	0.41	.12	5.84	+ .21	+ .046	.00
GY Sge	.708	(3.604)	1.11	.14	6.01	+ .14	- .006	.00
S Vol	1.826	(3.644)	0.77	1.15	-6.45	+0.24	+0.058	-0.05
				questionable cluster Cepheids				
V Cen	0.740	2.914	0.32	0.59	-3.68	-0.64	-0.066	-0.09
V367 Sct	0.799	3.386	(1.03)	.67	3.25	- .77	- .088	- .04
TW Nor	1.033	(3.477)	1.20	.83	4.18	- .40	- .123	+ .01
VX Per	.037	3.460	0.49	.75	4.42	- .41	- .048	- .08
RU Sct	.294	3.400	1.02	.76	5.46	- .43	- .022	- .19
SW Vel	.371	3.490	0.38	.87	5.43	- .40	- .014	+ .12
KQ Sco	.458	3.483	(0.99)	.99	5.94	+ .70	+ .037	- .04
RS Pup	1.617	3.327	0.52	0.97	-6.14	-0.42	-0.017	-0.14
				stars wrongly classified as cluster Cepheids				
CS Vel	0.771	(3.674)	0.68	0.69	-3.64	-1.31	-0.284	0.00
SX Vel	0.980	3.402	.28	.62	4.56	-0.93	- .082	- .18
SZ Cas	1.134	3.492	.85	.65	5.10	-0.86	- .082	- .22
V810 Cen	2.115	(3.733)	0.26	0.55	-9.54	-3.26	-0.245	-0.80

we got absolute magnitudes M_V which are also listed in Table 5, and then the M_V- $\log P$ relation. We assumed $R = 2.90$, as a value consistent with Eq. (7).

Consequently we can use three quantities as criteria for testing distances and photometric data of cluster Cepheids: ΔMod, $\Delta\log r$, and deviations from the $\langle B-V\rangle_0$- $\log P$ relation, denoted by $\Delta\langle B-V\rangle_0$. On the basis of the numerical results we propose to divide the investigated stars into three groups (Table 5):

(*a*) 21 stars with reliable distances and photometry, fulfilling three conditions:

$$|\Delta \text{Mod}| < 0.40,$$
$$|\Delta \log r| < 0.080,$$
$$|\Delta \langle B-V \rangle_0| < 0.08.$$

Omitting CF Cas a and CE Cas b, one gets the relations:

$$\begin{aligned} \langle B-V \rangle_0 &= 0.485 \log P + 0.317 \\ &\quad \pm .024 \qquad \pm .026 \\ \text{stand.dev.} &= 0.042 \end{aligned} \tag{21}$$

$$\begin{aligned} M_V &= -2.635 \log P - 1.494 \\ &\quad \pm .070 \qquad \pm .078 \\ \text{stand.dev.} &= 0.125 \end{aligned} \tag{22}$$

(*b*) 8 stars with questionable membership to this group, which fulfill only two or one from the above conditions.

(*c*) 4 stars with differences ΔMod, $\Delta \log r$, and $\Delta \langle B-V \rangle_0$ greater than the above limits or uncertain. They should not be regarded as typical, standard, cluster Cepheids.

As the consequence of Eqs. (12), (13), (21), and (22) also other parameters of cluster Cepheids are determined by the period P alone:

$$M_{bol} = -2.926 \log P - 1.247, \tag{23}$$

$$\log \mathcal{M}_{ph} = 0.514 \log P + 0.261. \tag{24}$$

Additional relations for the same group of stars result from the formulae given by Opolski and Ciurla (1984):

$$\begin{aligned} \log T_e &= 3.870 - 0.175 \langle B-V \rangle_0, \\ \log T_e &= -0.0848 \log P + 3.814. \end{aligned} \tag{25}$$

Surface brightness $S_V = 2.353 \langle B-V \rangle_0 + 3.182$,

$$S_V = 1.141 \log P + 3.928. \tag{26}$$

Radius R:

$$\begin{aligned} \log R &= 0.2 (S_V - M_V), \\ \log R &= 0.755 \log P + 1.084. \end{aligned} \tag{27}$$

In this group of stars $\log P$ varies from 0.290 for SU Cas to 1.826 for S Vul. Therefore other parameters of cluster Cepheids change in the ranges:

$$\begin{aligned} -2^{m}\!.26 &> M_V > -6^{m}\!.31, \\ -2.10 &> M_{bol} > -6.59, \\ 2.57 &< \mathcal{M}_{ph} < 15.8 \ M_\odot, \\ 20 &< R < 290. \end{aligned}$$

It is worth noticing that according to Eqs. (16) and (21) cluster Cepheids have $\langle B-V\rangle_0$ greater by about 0.05 in comparison with the mean values of the field Cepheids with the same periods. Therefore, cluster Cepheids remaining among the field stars in Fig. 7 are situated near the greatest $\langle B-V\rangle_0$ for a given $\log P$. Due to the value $\Delta\langle B-V\rangle_0 = 0.05$, the following other differences exist between cluster Cepheids and mean field Cepheids: lower temperatures $\Delta \log T_e = -0.009$, smaller luminosities $\Delta M_V = 0.14$, $\Delta M_{bol} = 0.11$, smaller masses $\Delta \log \mathcal{M}_{ph} = -0.09$ and smaller radii $\Delta \log R = -0.004$.

The next groups of stars have been selected on the basis of their position in the Galaxy and not according to their properties, as in the first group of cluster Cepheids. Different $\langle B-V\rangle_0$- $\log P$ relations have been found for stars in sectors limited approximately by galactic longitudes l: 0°, 90°, 270°, and 360° (see Fig. 4), except cluster Cepheids discussed above.

0° < l < 90°.

This group consists of 59 stars but E_{B-V} and consequently $\langle B-V\rangle_0$ are determined for only 32 of them (Table 6). From these values the following $\langle B-V\rangle_0$- $\log P$ relation has been calculated:

$$\begin{aligned} \langle B-V\rangle_0 &= 0.511 \;\log P + 0.295 \\ &\quad \pm .040 \qquad\quad \pm .035 \\ \text{stand.dev.} &= 0.042 \end{aligned} \tag{28}$$

Table 6

Cepheids in the area 0° < l < 90°.

Star	log P	$\langle B-V\rangle_0$	E_{B-V}	r_{kpc}	ΔV	
η Aql	0.856	0.69	0.14	0.29	0.80	
U "	0.847	.70	.36	0.70	.77	
SZ "	1.234	.92	.59	2.16	1.33	
TT "	1.138	.90	.46	1.10	1.18	
FF "	0.650	.59	.18	0.43	0.35	
FM "	.786	.66	.67	1.00	.72	
FN "	.977	.74	.52	1.66	.67	
PZ "	.942			5.µ3	.73	
V336 "	.864	.74	.64	2.26	.78	
V493 "	.475			2.23	.57	
V496 "	.833	.77	.41	1.06	.38	
V600 "	0.860	.70	.83	1.98	.66	
X Cyg	1.214	.98	.23	1.10	.99	clust.
SU "	0.585	.67	.12	0.98	.73	
SZ "	1.179			2.56	0.88	
TX "	1.168			1.60	1.22	
VX "	1.304			3.23	1.01	
VY "	0.895			2.37	0.83	
BZ "	1.006			2.53	0.52	
CD "	1.232	.95	.45	2.90	1.17	
DT "	0.398	.50	.05	0.44	0.29	
EP "	.632			6.84	.81	
EX "	0.686			4.95	.79	
EZ "	1.067			4.92	.78	
GH "	0.893			2.69	.76	
GI "	.762			4.00	.61	
MW "	.775			1.59	.70	
V383 "	.664			1.83	.55	
V386 "	.721			1.18	.71	
V402 "	.640			2.38	.56	
V532 "	.516			1.22	.34	
V547 "	.794			8.20	.96	
V924 "	0.746			5.25	.22	
Y Oph	1.234	.74	.64	0.81	.47	
BF "	0.609			0.84	.63	
AU Peg	.379			1.38	.40	
S Sge	.923	.74	.10	0.74	.76	
U Sgr	.829	.71	.43	0.68	.73	clust.
W "	.881	.64	.13	0.48	.77	
X "	.846	.53	.25	0.42	.61	
Y "	0.761	.71	0.18	0.54	0.71	
VY "	1.132	0.90	1.10	3.48	1.06	
WZ "	1.339	1.02	0.43	2.11	1.08	clust.
XX "	0.808			1.64	0.86	
YZ "	0.980	0.75	0.30	1.36	0.74	
AP Sgr	0.704	0.67	0.18	0.90	0.82	
AY "	.818	.72	.83	2.23	.82	
BB "	.822	.74	.28	0.89	.60	
V350 "	.712	.62	.33	1.00	.73	
X Sct	0.623	.57	.63	1.97	.91	
Y "	1.015	.84	.75	2.04	0.78	clust.
Z "	1.111	.91	.47	3.16	1.00	
RU "	1.294	.76	1.02	2.50	1.15	clust.?
SS "	0.565	.62	0.36	1.04	0.46	
TY "	1.044	.81	0.95	2.90	.88	
UZ "	1.169	.90	1.02	3.77	.93	
CK "	0.870	.79	0.83	2.34	.49	
CM "	.593			2.40	.70	
EV "	.490	.52	.64	1.71	.34	clust.
V367 "	.709			2.43	.49	clust.?
SR Ser	.724			1.87	.79	
T Vul	.647	.59	.07	0.60	.99	
U "	.903			0.73	.70	
X "	0.801	0.78	.70	1.12	0.76	
SV "	1.654	1.12	0.41	2.37	1.04	clust.

Three stars: Y Oph, X Sgr, and RU Scu were omitted as having $\langle B-V \rangle_0$ too small by 0.2.

The relation expressed by Eq. (28) is within the limits of accuracy identical with Eq. (21) valid for the cluster Cepheids. Therefore, the stars of this group are plotted in Fig. 8 together with the cluster Cepheids, in order to show that the cluster Cepheid line, Eq. (21), denoted c.C.l., fits well to the stars from sector $0° < l < 90°$. The masses of these stars are between 3.1 and 8.7 $M_\odot$.

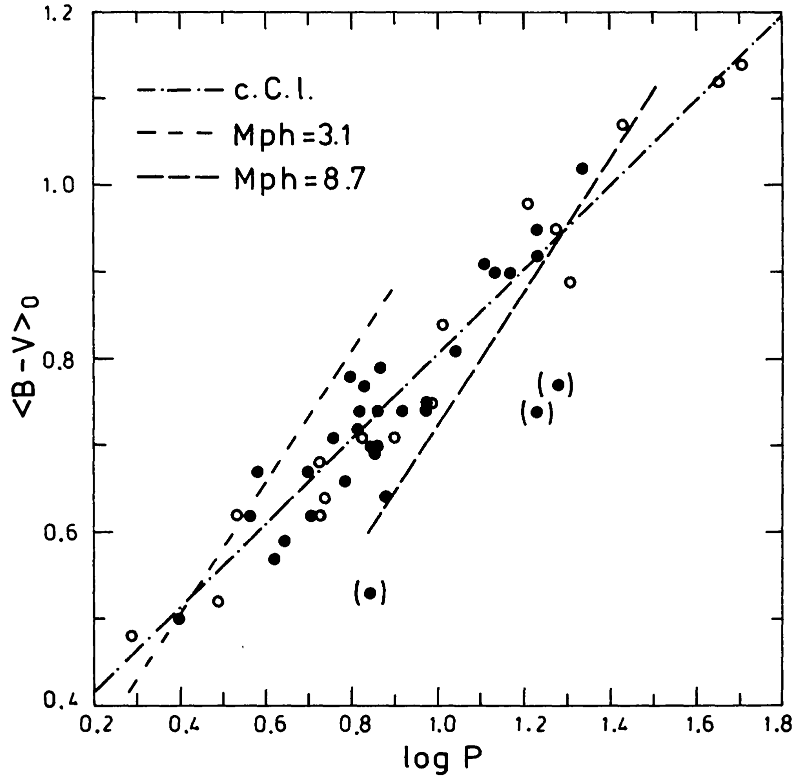

Fig. 8. The $\langle B-V \rangle_0$- $\log P$ diagram for cluster Cepheids indicated by open circles and determining the cluster Cepheid line, c.C.l., according to Eq. (21). Cepheids from the sector $0° < l < 90°$, filled circles, are near c.C.l. between constant mass lines 3.1 and 8.7 $M_\odot$. Three stars omitted in deriving Eq. (28) are in brackets.

The similarity of these two groups is also visible in Fig. 9, where the relation of light amplitude ΔV and $\langle B-V \rangle_0$ is shown. The stars of both groups are distributed in three areas limited by the lines plotted in Fig. 9 with maximum ΔV for $\langle B-V \rangle_0 = 0.9$. These limiting lines and cluster Cepheid line, c.C.l., will be repeated in next figures in order to facilitate the comparison of Cepheid properties in different regions of the Galaxy.

$90° < l < 270°$ + strip: $0 < X < 0.2$ kpc, $Y < 0$.

The stars in the galactic anticenter direction and in the strip 0.2 kpc wide, directed towards negative Y, form a separate group (Table 7). 58 of them have known $\langle B-V \rangle_0$ values, which are used in Fig. 10 to show the $\langle B-V \rangle_0$- $\log P$ relation. The cluster Cepheid line, c.C.l., from Fig. 8 in also plotted as a

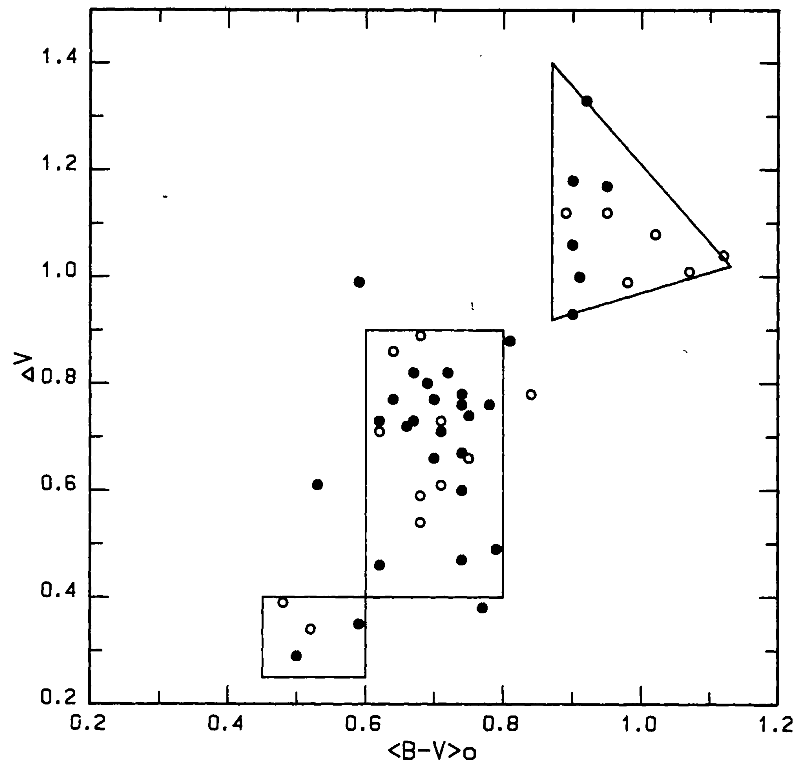

Fig. 9. The ΔV-$\langle B-V\rangle_0$ diagram for cluster Cepheids indicated by open circles and for Cepheids in the sector $0° < l < 90°$, filled circles.

reference line. As one can see the c.C.l. fits these stars only in the range $0.5 < \log P < 0.8$. For longer periods, the $\langle B-V\rangle_0$ values are systematically smaller. Exceptions are Z Lac (1.04, 0.90) and 1 Car (1.55, 1.10) which are near the c.C.l. and VZ Pup (1.36, 0.72) which has large negative $Z = -354$ pc. Omitting these exceptions and the cluster Cepheids we obtain the relation:

$$\langle B-V\rangle_0 = 0.360 \log P + 0.371. \qquad (29)$$
$$\pm .030 \qquad \pm .026$$
$$\text{stand.dev.} = 0.056$$

The masses for the second crossing stars in this group are from 2.7 to 22.6 $M_\odot$.

Figure 11 shows that amplitudes ΔV and $\langle B-V\rangle_0$ values are only partly consistent with limits determined previously in Fig. 9. Some of these stars have greater amplitudes or smaller $\langle B-V\rangle_0$.

$270° < l < 360°$ – strip $0 < X < 0.2$ kpc, $Y < 0$.

In this part of the Galaxy it is possible to separate the interarm stars discussed previously and situated in the area: $0.2 < X < 1.3$ kpc, $-3.0 < Y < 0.0$ kpc and to regard them as a special subgroup.

The remaining 29 stars of this area with known $\langle B-V\rangle_0$ have periods

Table 7

Cepheids in the area $90^\circ < l < 270^\circ$ and $0 < X < 0.2$ kpc., $Y < 0$.

Star	log P	$\langle B-V \rangle_0$	E_{B-V}	r_{kpc}	ΔV	
Y Aur	0.586			2.12	0.82	
RT "	0.572	0.58	0.06	0.46	.80	
RX "	1.065	.73	.26	2.01	.69	
SY "	1.006	.68	.40	3.03	.62	
YZ "	1.260			5.38	.99	
AN "	1.012			4.68	.67	
BK "	0.93			2.95	.69	
RW Cam	1.215	.89	.53	2.37	.91	
RX "	0.898	.72	.55	1.01	.77	
AB "	0.762			5.66	.98	
RY CMa	0.670	.69	.20	1.33	.74	
RZ "	0.629	.52	.52	2.12	.61	
SS "	1.092	.72	.56	3.98	.99	
TV "	0.669	.67	.58	2.58	.80	
TW "	0.845	0.62	.40	3.09	.65	
Car	1.551	1.10	.21	0.53	.75	
V "	0.826	0.67	.22	1.28	.60	
RS Cas	0.799			1.75	0.78	
RW "	1.170			3.24	1.14	
RY "	1.084			3.42	0.97	
SU "	0.290	.48	.24	0.24	0.31	clust.
SW "	0.736			2.25	.67	
SY "	0.610			2.30	.80	
SZ "	1.134	.65	.85	3.10	.41	
TU "	0.330	.42	.19	0.87	.82	2-mod.
UZ "	.629			4.22	.76	
VV "	.793			3.95	.89	
VW "	.778			3.36	.67	
XY "	.653			2.17	.57	
AP "	.836			4.43	.62	
AY "	.458			2.61	.62	
BP "	.797			2.60	.77	
BY "	.508			1.59	.37	
CD "	.892			3.11	.78	
CE " a	.711			3.45	.52	clust.
CE " b	.651			3.51	.68	clust.
CF "	.688	.68	.55	3.54	.54	clust.
CG "	0.640			3.42	0.83	
CH "	1.178			4.43	1.08	
CY "	1.158			5.41	1.10	
CZ "	0.753			4.00	0.80	
DD "	.992			3.44	.59	
DF "	.584			2.77	.60	
DL "	.903	0.71	0.51	1.98	.61	clust.
DW "	0.699			2.62	0.59	
FM Cas	0.764			2.09	0.57	
Cep	.730	0.68	0.09	0.28	.85	
AK "	0.859			4.27	.66	
CP "	1.252			4.26	.90	
CR "	0.795			1.57	.37	
VZ Cyg	.687			1.96	.66	
V459 "	.860			2.79	.71	
V538 "	.767			2.77	.51	
Dor	0.993	.72	.10	0.36	.62	
Gem	1.006	.80	.03	0.39	.50	
W "	0.898	.71	.25	1.09	.83	
RZ "	0.743			2.74	.89	
AA "	1.053			4.18	.67	
AD "	0.578			3.17	.64	
V Lac	.698	.69	.26	1.91	.97	
X "	.736	.66	.29	1.62	.40	
Y "	.636	.59	.18	2.39	.65	
Z "	1.037	.90	.29	2.08	.92	
RR "	0.807	.68	.27	2.26	.79	
BG "	.727	0.69	.30	1.86	.63	
DF "	0.651			4.92	0.67	
T Mon	1.432	1.07	.18	1.38	1.01	clust.
SV "	1.183	0.88	.24	2.75	1.28	
TX "	0.940	.63	.54	5.70	0.64	
TZ "	.871	.77	.41	4.51	.72	
WW "	.669			7.06	.94	
XX "	.737	.56	.64	5.75	.69	
AC "	.904	.70	.50	3.35	.69	
CS "	.828	.62	.58	4.47	.57	
CU "	.673			8.25	.70	
CV "	.731	.62	.75	2.19	.71	clust.
EK "	.598	.68	.56	2.90	.64	
RS Ori	.879	.64	.37	1.94	.80	
CR "	.691			6.79	.58	
CS "	0.590			4.83	.86	
SV Per	1.046	.69	.37	3.21	.79	
SX "	0.632			3.46	.80	
UX "	.660			5.52	.95	
UY "	0.730	.68	.91	2.58	.89	clust.
VX "	1.037	.75	0.49	2.89	.70	clust.?
VY "	0.743	.64	1.00	2.33	.86	clust.
AS "	.697			1.49	.96	
AW "	.810	.65	0.46	0.97	.81	
DW "	0.562			3.69	0.66	
X Pup	1.414	0.89	0.43	3.68	1.42	
RS Pup	1.617	0.97	0.52	2.12	1.09	clust.?
VW "	0.632	.67	.48	4.00	0.71	
VX "	0.479			1.42	0.73	2-mod.
VZ "	1.365	.72	.53	6.10	1.40	
WW "	0.742	.55	.39	4.45	0.96	
WX "	.951	.72	.32	2.89	.57	
WY "	.720	.58	.27	4.88	.78	
WZ "	0.701			4.37	0.90	
AD "	1.133	.79	.36	5.08	1.05	
AP "	0.706	.66	.22	1.07	0.68	
AQ "	1.475	.93	.53	3.87	1.28	
AT "	0.824	.59	.22	1.88	0.87	
ST Tau	.606			1.21	.77	
SZ "	.498	.55	.31	0.50	.34	
α UMi	.599	.59	.00	0.10	.19	
T Vel	.666	.60	.30	1.25	.64	
V "	0.641	.53	.28	1.11	0.73	
RZ "	1.310	.89	.32	1.83	1.22	clust.
ST "	0.768	.70	.54	2.12	0.68	
SW "	1.371	.87	.38	3.09	1.53	clust.?
SX "	0.980	.62	.29	2.53	0.68	
AH "	.626	.57	.03	0.60	.37	
AP "	.495	.61	.46	1.84	.92	2-mod.
AX "	.414	.48	.24	1.11	.44	2-mod.
BG "	0.840	.72	.48	0.98	.48	
DR "	1.049	0.83	0.75	2.11	0.57	

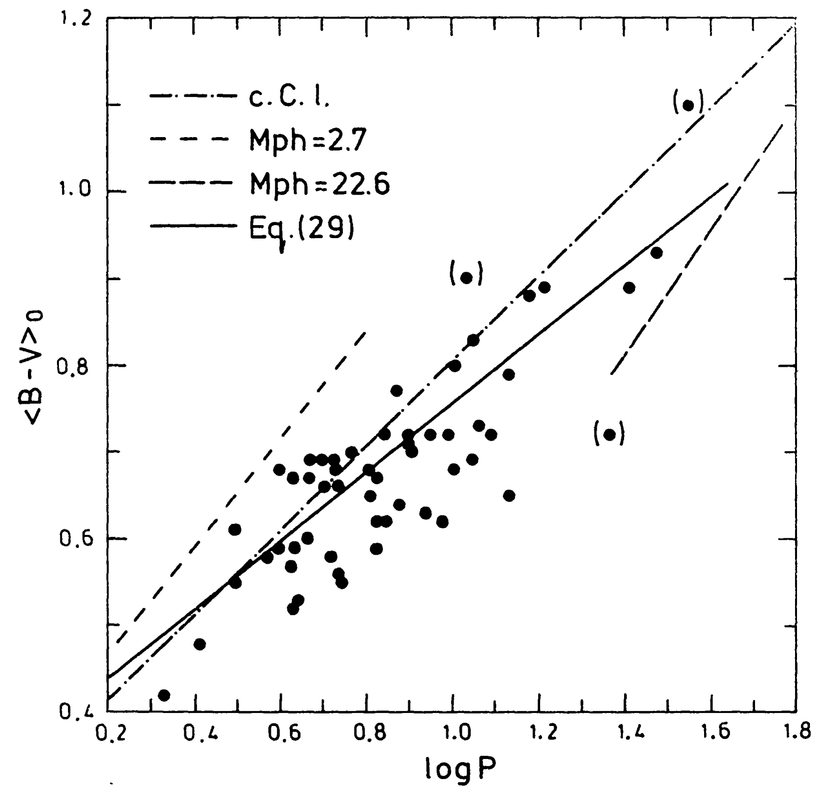

Fig. 10. The $\langle B-V\rangle_0$-log P diagram for Cepheids $90° < l < 270°$ and in the strip $0 < X < 0.2$ kpc, $Y < 0$. The stars are between constant mass lines 2.7 and 22.6 $M_\odot$. Cluster Cepheid line, c.C.l. and the line representing Eq. (29) are also indicated. Three stars omitted in deriving Eq. (29) are in brackets.

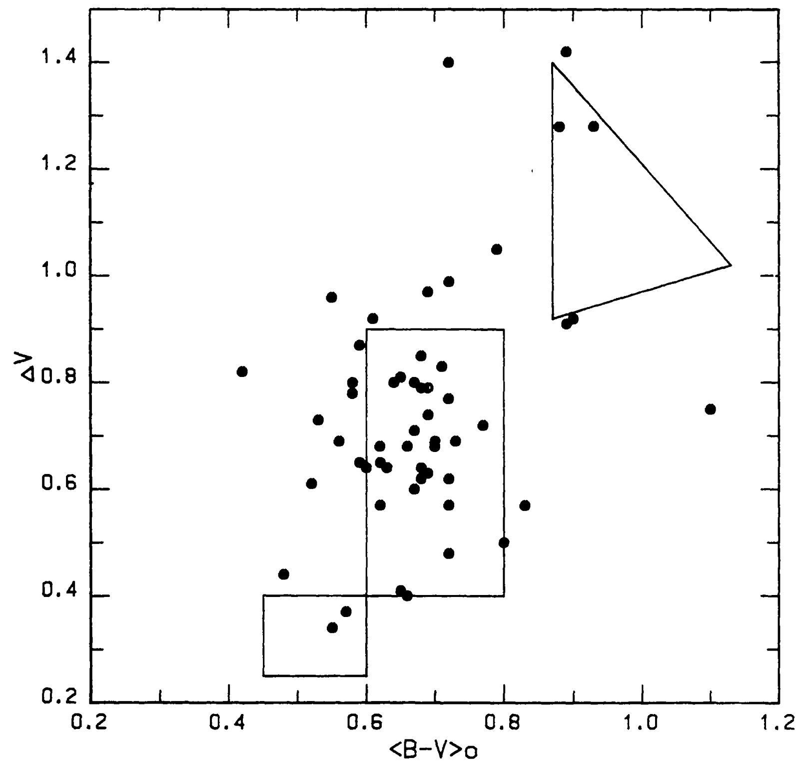

Fig. 11. The ΔV-$\langle B-V\rangle_0$ diagram for Cepheids in the area $90° < l < 270°$ and in the strip $0 < X < 0.2$ kpc., $Y < 0$.

$0.6 < \log P < 1.5$ (Table 8) and satisfy the relation:

$$\langle B-V \rangle_0 = \underset{\pm .040}{0.219} \log P + \underset{\pm .043}{0.519} \qquad (30)$$

$$\text{stand.dev.} = 0.046$$

Omitted are FI Car and VW Cen with greater and U Nor with smaller $\langle B-V \rangle_0$ values (Fig. 12). In comparison with the cluster Cepheid line, stars

Table 8

Cepheids in the area $270° < l < 360°$ without strip $0 < X < 0.2$ kpc, $Y < 0$ and without the interarm area.

Star	log P	$\langle B-V \rangle_0$	E_{B-V}	r_{kpc}	ΔV	
WZ Car	1.362	0.83	0.41	5.27	1.32	
XX "	1.196	.74	.38	4.67	1.22	
XY "	1.095	.79	.44	3.26	0.83	
YZ "	1.259	.73	.42	3.73	.81	
AO "	0.990	.74	.21	3.16	.59	
CC "	0.678	.65	.58	5.27	.58	
CN "	0.693	.73	.41	3.30	.70	
CR "	0.990	.77	.56	6.74	.56	
DY "	0.670			4.65	.69	2-mod.
FI "	1.129	.92	.70	6.13	.59	
FN "	0.661	.57	.58	4.69	.66	
FO "	1.015	.77	.52	5.13	.60	
FR "	1.030	.71	.46	3.72	0.68	
TX Cen	1.233	0.88	.89	3.61	1.30	
VW "	1.177	1.02	.38	4.62	1.02	
KK "	1.086	0.81	.56	7.31	0.98	
KN "	1.532	.87	.73	5.73	1.07	
KZ "	0.182			6.22	0.97	
V339 "	0.976	.78	.44	2.00	.77	
AO "	0.806	.64	.68	3.76	.74	
TZ Mus	0.694			3.90	0.64	2-mod.
UU "	1.066	.76	0.42	4.14	1.03	
U Nor	1.102	.60	1.04	1.85	0.97	
RS "	0.792	.76	0.56	2.28	.71	
SY "	1.102	.72	.66	2.98	.89	
GU "	0.538	.68	.62	1.76	.59	clust.
BF Oph	0.609	.62	.28	0.84	.63	
RY Sco	1.308	.80	.68	1.90	.92	
KQ "	1.458			3.04	.95	clust.?
V500 "	0.969	.69	.62	1.81	.73	
RY Vel	1.449	.79	.60	3.30	.89	
XX "	0.844	.69	.54	3.86	.97	
OD "	1.120			8.21	.60	
DP "	0.739			4.05	.69	
EX "	1.122	.74	.87	6.29	.84	
FG "	0.810	0.75	0.85	3.76	0.59	

determining relation (30) are placed near this line only for $0.6 < \log P < 0.9$. According to small slope of relation (30) the stars with longer periods are below the c.C.l. The masses are from 3.0 to 28 $M_\odot$.

In Fig. 13 we represent the ΔV - $\langle B-V \rangle_0$ relation. All stars have ΔV greater than 0.55 and $\langle B-V \rangle_0$ greater than 0.57, due to their long periods. But the distribution of these values differs from limits accepted on Fig. 9.

The interarm area: $0.2 < X < 1.3$ kpc, $-3.0 < Y < 0.0$ kpc.

These stars are listed in Table 9. Fig. 14 shows that they are gathered in short period range from $\log P = 0.4$ to 0.9. Only 6 scattered ones have longer

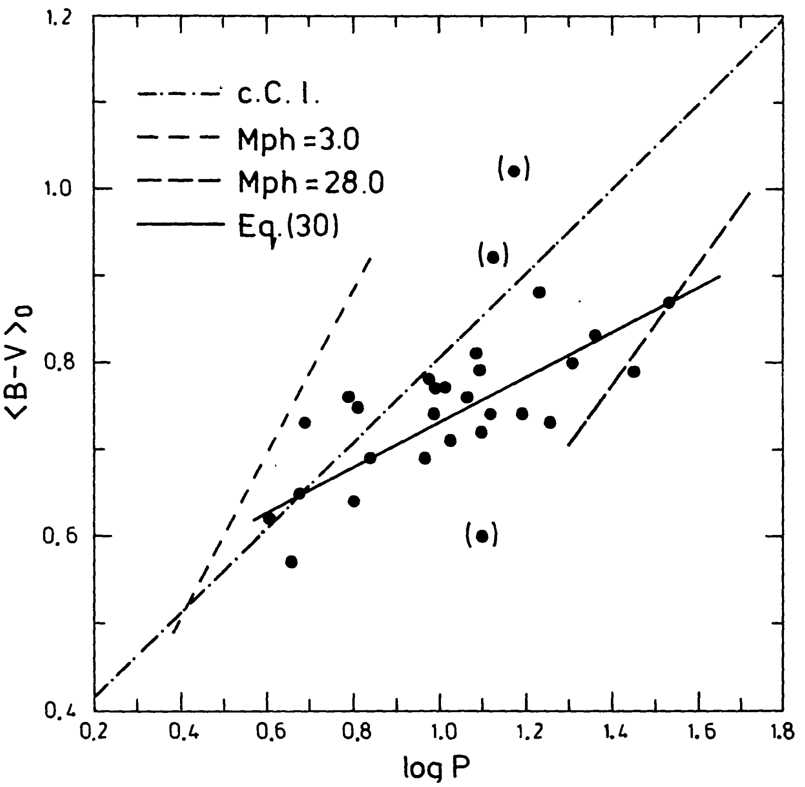

Fig. 12. The $\langle B-V\rangle_0$-$\log P$ diagram for Cepheids in the area $270° < l < 360°$ without strip $0 < X < 0.2$ kpc, $Y < 0$ and without the interarm area $0.2 < X < 1.3$ kpc, $-3.0 < Y < 0$ kpc. The stars are between constant mass lines 3.0 and 28.0 $M_{\odot}$. Cluster Cepheid line, c.C.l., and line representing Eq. (30) are indicated. Three stars omitted in deriving Eq. (30) are in brackets.

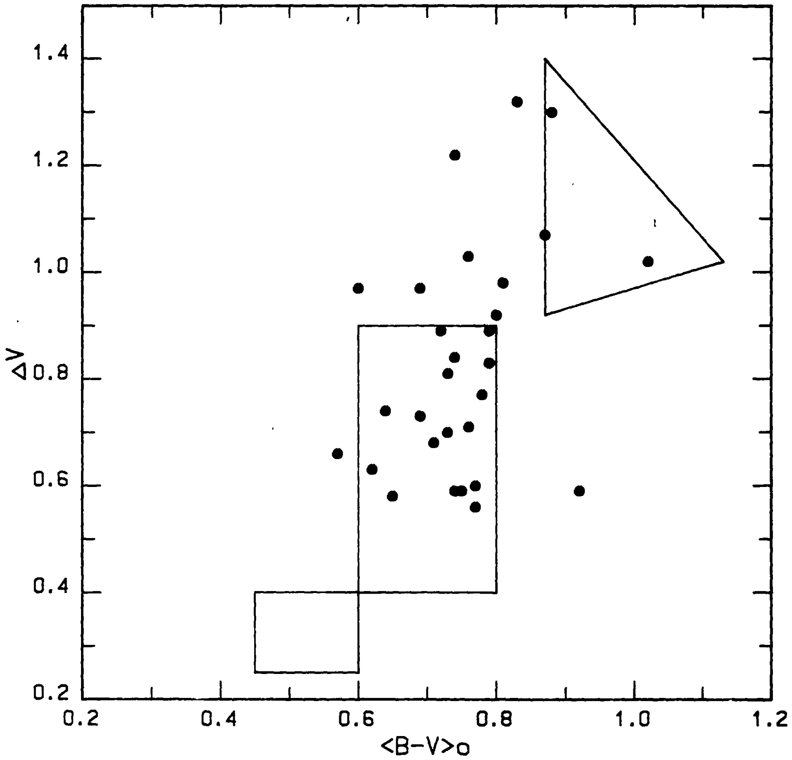

Fig. 13. The ΔV-$\langle B-V\rangle_0$ diagram for Cepheids in the area $270° < l < 360°$ without strip $0 < X < 0.2$ kpc, $Y < 0$ and without interarm Cepheids.

Table 9

Cepheids in the interarm area $0.2 < X < 1.3$ kpc. $-3.0 < Y < 0$ kpc.

Star	log P	$\langle B-V\rangle_0$	E_{B-V}	r_{kpc}	ΔV	
U Car	1.588	0.96	0.30	1.95	1.22	
Y "	0.561	.48	.16	1.55	0.59	2-mod.
SX "	.687	.58	.35	2.10	.75	
UW "	.728	.57	.46	2.31	.85	
UX "	.566	.55	.14	1.59	.81	
UY "	.744	.64	.22	2.34	.76	
UZ "	0.716			2.53	0.60	
VY "	1.277	.95	.24	2.05	1.12	clust.
WW "	0.670	.49	.43	2.74	0.76	
XZ "	1.221	.92	.37	2.75	1.08	
CY "	0.630			2.43	0.52	
ER "	.888	.73	.14	1.14	.52	
EY "	.459			2.67	.49	2-mod.
GH "	.758	.58	.39	2.32	.34	
GI "	.646	.50	.25	1.70	.30	
GX "	.857	.70	.40	2.52	.80	
GZ "	.619	.59	.41	2.78	.30	2-mod.
IT "	.877	.77	.23	1.73	.36	
V Cen	.740	.59	.32	0.82	.78	clust.?
UZ "	0.523	.53	.26	1.59	.77	2-mod.
XX "	1.040	.71	.30	2.00	.89	
AY "	0.725			1.76	.58	
AZ "	.507	.49	.20	1.65	.31	
BB "	.602	.60	.35	2.79	.58	
BK "	.502			2.31	.69	2-mod.
MY Cen	.570			2.16	.96	
V378 "	.810	.54	.49	1.69	.39	
V381 "	.706	.60	.22	1.29	.69	
V419 "	.741	.60	.20	1.801	.29	
V496 "	.646	.63	.58	1.96	.62	
AX Cir	.722			0.66	.44	
R Cru	.765	.63	.19	0.96	.82	
S "	.671	.61	.20	0.75	.69	
T "	.828	.74	.20	0.84	.47	
X "	0.794	.72	0.30	1.62	.59	
SU "	1.109	.72	1.08	1.97	.68	
VW "	0.721	.75	0.58	1.66	.60	
AG "	.584	.54	.26	1.36	.81	
R Mus	.876	.65	.14	0.99	.80	
S "	0.985	0.56	0.28	1.04	0.54	
RT Mus	0.489	0.52	0.37	1.44	0.73	
S Nor	.989	.75	.22	1.01	.66	clust.
IQ "	.916			1.45	.64	
RV Sco	.738	.63	.38	0.87	.87	
V482 "	.656	.67	.34	1.05	.67	
V636 "	.832	.72	.22	0.87	.53	
R TrA	.530	.48	.27	0.65	.54	
S "	.801	.68	.10	0.90	.79	
U "	0.410	.51	.13	1.07	0.77	2-mod.
SV Vel	1.149	.70	.44	2.90	1.14	
AE "	0.853	0.63	0.66	3.00	0.85	

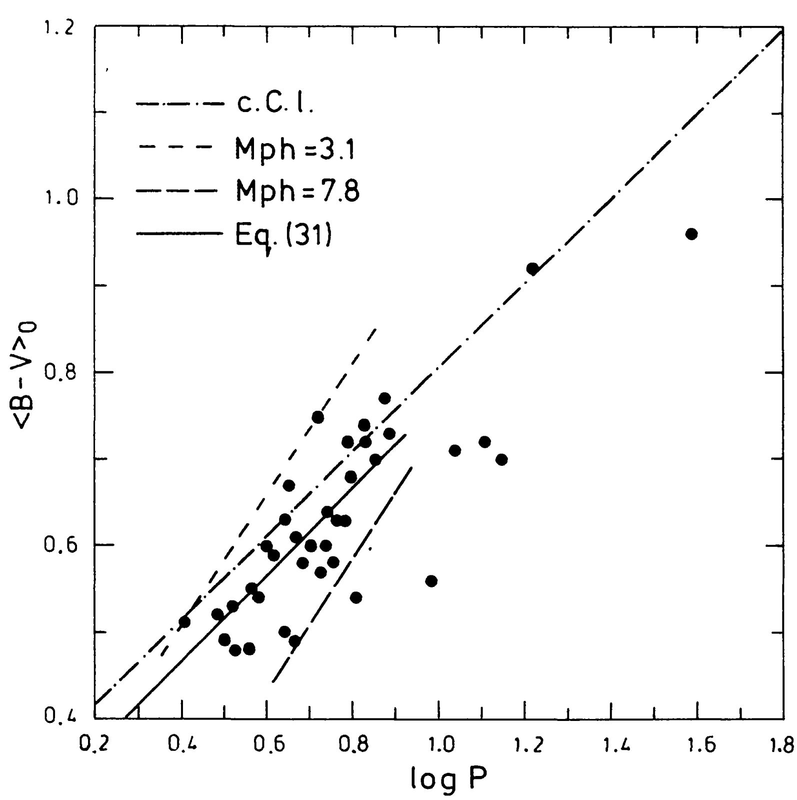

Fig. 14. The $\langle B-V\rangle_0$-log P diagram for interarm Cepheids, $0.2 < X < 1.3$ kpc, $-3.0 < Y < 0.0$ kpc. Short period stars $0.4 < \log P < 0.9$ are between constant mass lines 3.1 and 7.8 $M_\odot$ and determine Eq. (31). Cluster Cepheid line, c.C.l., is plotted as a reference line.

periods. The short period body of these stars is placed between constant mass lines 3.1 and 7.8 $M_{\odot}$. The $\langle B-V\rangle_0$- $\log P$ relation obtained from 35 stars with $0.4 < \log P < 0.9$ is:

$$\langle B-V\rangle_0 = \underset{\pm .055}{0.503} \log P + \underset{\pm .054}{0.255}. \tag{31}$$

$$\text{stand.dev.} = 0.055$$

In Fig. 14 this relation is represented as a line parallel to the c.C.l., shifted by 0.05 towards smaller $\langle B-V\rangle_0$.

The ΔV- $\langle B-V\rangle_0$ relation for interarm stars (Fig. 15) is characterized by the same values of amplitudes as indicated by the limits, but in the range

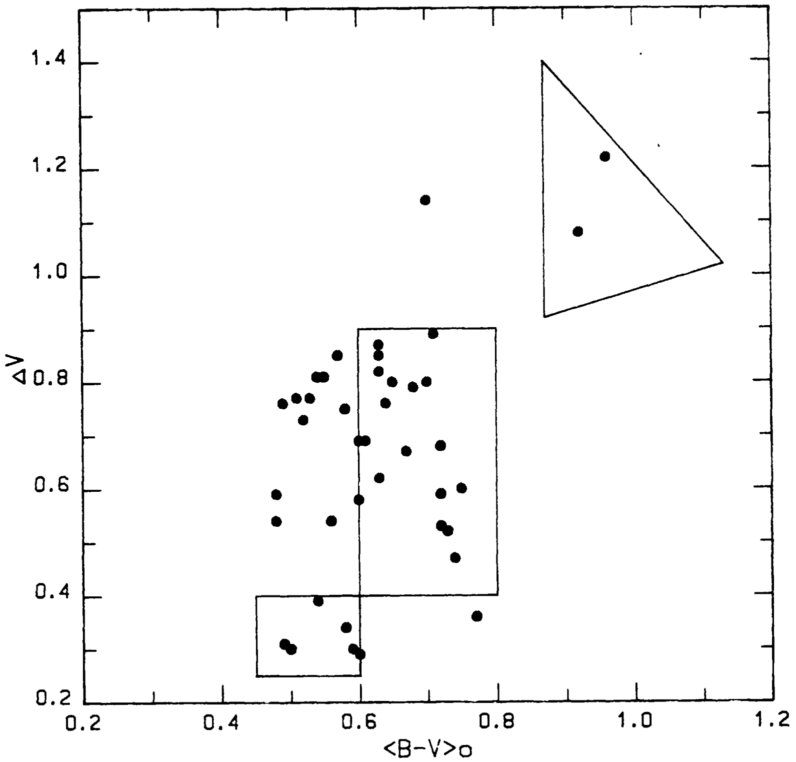

Fig. 15. The ΔV-$\langle B-V\rangle_0$ diagram for interarm Cepheids.

$0.5 < \Delta V < 0.9$ connected partly with the smaller $\langle B-V\rangle_0$ values. Well represented are small amplitudes, $0.25 < \Delta V < 0.40$ for $0.45 < \langle B-V\rangle_0 < 0.60$. It is worth notice that six double-mode Cepheids, from twelve occurring in ST catalogue, are situated in this small interarm area.

Some additional differences between the above discussed groups can be also noticed, when we take into consideration all type I stars of the ST catalogue, with and without known $\langle B-V\rangle_0$. The percentages of short- and long-period stars in groups are given in Table 10. We see that the interarm region is exceptionally rich in short-period stars, 90%, whereas the remaining

Table 10
Percentage of long- and short-period Cepheids.

	N	$\log P < 1$	$\log P > 1$
1. Cluster Cepheids	19	63%	37%
2. $0° < l < 90°$	59	76	24
3. $90° < l < 270°$	104	75	25
4. $270° < l < 360°$	35	46	54
5. Interarm	49	90	10

space of the 270°–360° quadrant has the increased percentage of longperiod stars, 54%. In other groups these ratios are about 75:25.

Similarly we can compare the amplitudes ΔV distribution. In order to liberate the results from the dependence of amplitudes on periods, we consider the stars from the period range $0.6 < \log P < 0.9$ only. The results are given in Table 11. Here we see again that the interarm region is standing out as having the highest percentage of small amplitudes with a complete lack of large ones.

Table 11
Amplitude distribution of Cepheids.

	N	ΔV: 0.2 – 0.5	0.5 – 0.9	> 0.9
1. Cluster Cepheids	6	0%	100%	0%
2. $0° < l < 90°$	31	16	74	10
3. $90° < l < 270°$	59	8	80	12
4. $270° < l < 360°$	10	0	90	10
5. Interarm	31	26	74	0

As a recapitulation we may state that the investigated properties of Cepheids depend on their position in the Galaxy, but on the basis of available data it is not possible to draw convincing conclusions about their relation to the spiral structure. One exception is the interarm area, $0.2 < X < 1.3$ kpc, $-3.0 < Y < 0$ kpc, which in many respects differs from other regions. The differences are also observable among the long-period stars, due the changes of the slopes in the $\langle B-V \rangle_0$-$\log P$ relations. In the quadrant 0°–90°, the long-period Cepheids have relatively large $\langle B-V \rangle_0$ values, similarly as the cluster Cepheids. Consequently, they have lower temperatures and smaller masses than the long-period stars with larger amplitudes in the quadrant 270°–360°. This may be connected with the changes of the stellar properties along the spiral arms. Quadrant 0°–90° is closer to the beginnings of arms than quadrant 270°–360°.

The author expresses gratitude to Dr. Tadeusz Ciurla for performing the calculations and for inspiring discussions.

REFERENCES

Dean, J. F., Warren, P. R., and Cousins, A. W. J. 1978, *M.N.R.A.S.*, **183**, 569.
Downes, D., Güsten, R. 1982, *Mitt. Astron. Ges.* Nr. 57, p. 207.
Efremov, Yu. N., Ivanov, G. R., and Nikolov, N. S. 1981, *Astroph. Space Sci.*, **75**, 407.
Fernie, J. D., and McGonegal, R. 1983, *Ap. J.*, **275**, 732.
Fernie, J. D., and Hube, J. O. 1968, *Astr. J.*, **73**, 492.
Gieren, W. P. 1986, *Ap. J.*, **306**, 25.
Ivanov, G. R., Efremov, Yu. N., and Nikolov, N. S. 1983, *Var. Stars*, **21**, 861.
Mihalàs, D., Binney, J. 1981, *Galactic Astronomy* (W. H. Freeman and Co., San Francisco).
Moffett, T. J., and Barness III, T. G. 1985, *Ap. J. Suppl.*, **58**, 843.
Opolski, A. 1984, *Acta Astr.*, **34**, 225.
– 1985, *Inf. Bull. Var. Stars*, No. 2688.
Opolski, A., and Ciurla, T. 1984, *Inf. Bull. Var. Stars*, No. 2528.
Pel, J. W. 1978, *Astr. Astrophys.*, **62**, 75.
Schaltenbrand, R., and Tammann, G. A. 1971, *Astr. Astrophys. Suppl. Ser.*, **4**, 265.
van Genderen, A. M. 1983, *Astr. Astrophys.*, **124**, 223.